Supplemental information for "**Energy production advantage of independent subcell connection for multijunction photovoltaics**"

The spectrum splitting ensembles used in this analysis are composed of ideal cells with 2 to 20 subcells. The subcells are either connected in electrical series, necessitating current matching through all subcells, or they are treated as electrically independent. The series-connected ensembles were optimized using Henry's method, which breaks the spectrum into bands of equal flux. In this procedure, the bandgaps of all subcells are determined by the top subcell bandgap (for a given input spectrum), and the ensembles are optimized by comparing the performance for a range of top subcell bandgap values. The subcell bandgaps for the series-connected ensembles are listed in Table 1.

Table 1. Bandgap values for series connected spectrum splitting ensembles

2	3	4	5	6	7	8	9	10	11	12	13	14	15	16	17	18	19	20
0.95	0.93	0.75	0.70	0.71	0.72	0.54	0.56	0.57	0.52	0.53	0.55	0.55	0.59	0.53	0.55	0.54	0.58	0.52
1.57	1.33	1.12	0.98	0.95	0.93	0.75	0.75	0.75	0.70	0.70	0.71	0.70	0.73	0.60	0.69	0.60	0.71	0.58
	1.85	1.48	1.25	1.18	1.13	0.97	0.95	0.93	0.79	0.78	0.79	0.77	0.79	0.74	0.75	0.74	0.76	0.71
		1.96	1.60	1.44	1.33	1.16	1.11	1.05	0.98	0.96	0.96	0.93	0.95	0.80	0.81	0.79	0.81	0.76
			2.06	1.74	1.56	1.37	1.26	1.21	1.13	1.07	1.05	1.02	1.02	0.96	0.96	0.93	0.96	0.81
				2.17	1.85	1.59	1.47	1.39	1.26	1.21	1.18	1.14	1.14	1.04	1.03	1.00	1.01	0.96
					2.26	1.88	1.69	1.56	1.44	1.36	1.29	1.23	1.22	1.15	1.14	1.07	1.10	1.01
						2.28	1.96	1.77	1.60	1.50	1.44	1.38	1.35	1.23	1.22	1.18	1.18	1.10
							2.35	2.03	1.81	1.67	1.58	1.49	1.46	1.36	1.32	1.25	1.25	1.18
								2.41	2.07	1.87	1.75	1.64	1.57	1.47	1.43	1.37	1.36	1.25
									2.44	2.12	1.93	1.79	1.71	1.58	1.53	1.46	1.44	1.36
										2.48	2.18	1.98	1.86	1.72	1.65	1.56	1.53	1.44
											2.53	2.22	2.04	1.87	1.78	1.68	1.64	1.53
												2.56	2.28	2.05	1.92	1.81	1.75	1.64
													2.60	2.28	2.10	1.95	1.87	1.75
														2.61	2.33	2.12	2.01	1.87
															2.64	2.35	2.18	2.01
																2.66	2.39	2.18
																	2.69	2.39
																		2.69

The ensembles with electrically independent subcells are not constrained to have equal current in all subcells, which increases the design space geometrically with the number of subcells. These ensembles with optimized through a simulated annealing process. The optimization began with a randomly seeded band gap combination. For each step, a random fluctuation was applied to each bandgap in the ensemble, the efficiency of the perturbed ensemble calculated and the perturbed efficiency compared to the best ensemble efficiency achieved to that point. If the perturbed efficiency was higher, the perturbed ensemble was adopted as the new best ensemble and its bandgap values served as the base for the next step. Otherwise the previous best ensemble remained as the base. In order to ensure the design space was widely sampled, a lower performing perturbed ensemble would still be adopted as the new base (while retaining the actual highest performing ensemble information) if its efficiency was within a window below the actual best efficiency. The window was wide for early optimization steps to allow wide sampling and narrowed as the optimization progressed to focus on finding the true maximum. For this analysis the simulated annealing was performed in two stages: one where all bandgaps in the ensemble were perturbed simultaneously and a second where one bandgap at a time fluctuated. The two stages were repeated 6-8 times for each number of bandgaps in search of repeated values, which were taken as indicative of a global optimum. The subcell bandgaps for the electrically independent ensembles are listed in Table 2.

Table 2. Bandgap values for spectrum splitting ensembles with electrically independent subcells

2	3	4	5	6	7	8	9	10	11	12	13	14	15	16	17	18	19	20
0.94	0.94	0.7	0.7	0.69	0.69	0.69	0.69	0.69	0.53	0.51	0.51	0.52	0.51	0.53	0.53	0.52	0.51	0.52
1.64	1.39	1.12	1	0.94	0.94	0.94	0.93	0.93	0.7	0.7	0.7	0.7	0.7	0.69	0.7	0.69	0.62	0.59
	2	1.55	1.38	1.17	1.13	1.15	1.13	1.13	0.93	0.93	0.93	0.94	0.92	0.77	0.79	0.75	0.69	0.69
		2.1	1.81	1.51	1.39	1.38	1.33	1.33	1.13	1.13	1.11	1.13	0.98	0.92	0.94	0.93	0.75	0.75
			2.33	1.94	1.71	1.63	1.55	1.55	1.33	1.36	1.24	1.33	1.13	1	1.12	1.11	0.94	0.93
				2.55	2.01	1.87	1.73	1.74	1.52	1.55	1.38	1.51	1.37	1.11	1.3	1.2	1.11	1.02
					2.44	2.21	1.91	2.02	1.71	1.74	1.55	1.67	1.51	1.19	1.39	1.38	1.18	1.15
						2.64	2.23	2.29	1.86	2	1.71	1.83	1.6	1.33	1.52	1.55	1.24	1.25
							2.61	2.67	2.09	2.35	1.83	2	1.77	1.46	1.67	1.71	1.38	1.38
								3.25	2.38	2.55	2.01	2.23	2.01	1.63	1.8	1.83	1.55	1.55
									2.91	2.81	2.25	2.61	2.19	1.8	2	2.01	1.73	1.67
										3.13	2.48	2.88	2.33	1.92	2.25	2.14	1.91	1.74
											2.93	3.1	2.55	2.09	2.41	2.35	2	1.86
												3.32	2.92	2.27	2.61	2.48	2.1	2
													3.31	2.59	2.86	2.55	2.3	2.14
														3	3.03	2.88	2.47	2.4
															3.44	3.02	2.78	2.59
																3.36	3.18	2.78
																	3.31	3.09
																		3.39

Figure 2 in the manuscript shows the results of an analysis of the average efficiency of the spectrum splitting ensembles under spectra for Phoenix, AZ that fall into different power ranges. The spectra that fall in those power ranges are plotted in Figure 1.

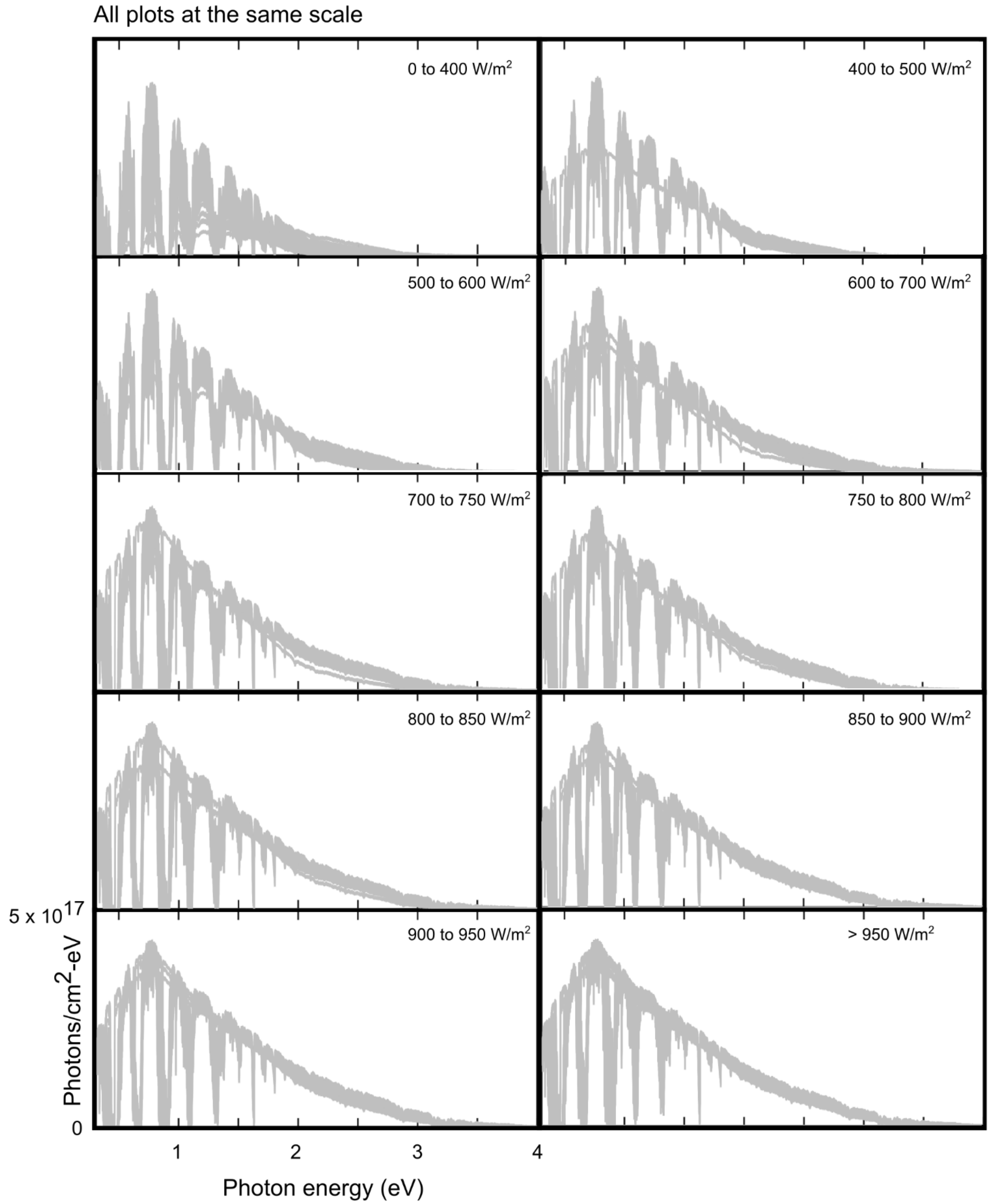

Figure 1. Spectra generated for Phoenix, AZ sorted by cumulative irradiance level. The average performance of the spectrum splitting ensembles under these ten sets of spectra were used to generate Figure 2 in the main text.